nature materials

SUPPLEMENTARY INFORMATION

https://doi.org/10.1038/s41563-020-0732-6

In the format provided by the authors and unedited.

Configurable phonon polaritons in twisted α-MoO_3

Mingyuan Chen[1,4], Xiao Lin[2,4], Thao H. Dinh[3], Zhiren Zheng[3], Jialiang Shen[1], Qiong Ma[3], Hongsheng Chen[2], Pablo Jarillo-Herrero[3] and Siyuan Dai[1]✉

[1]Materials Research and Education Center, Department of Mechanical Engineering, Auburn University, Auburn, AL, USA. [2]Interdisciplinary Center for Quantum Information, State Key Laboratory of Modern Optical Instrumentation, ZJU-Hangzhou Global Science and Technology Innovation Center, Zhejiang University, Hangzhou, China. [3]Department of Physics, Massachusetts Institute of Technology, Cambridge, MA, USA. [4]These authors contributed equally: Mingyuan Chen, Xiao Lin. ✉e-mail: sdai@auburn.edu

Configurable phonon polaritons in twisted α-MoO_3

M. Chen[1†], X. Lin[2†], T. Dinh[3], Z. Zheng[3], J. Shen[1], Q. Ma[3], H. Chen[2], P. Jarillo-Herrero[3], S. Dai[1]*

S1. Twisting configuration revealed in s-SNOM images at 910 cm^{-1} and 915 cm^{-1}

The s-SNOM images at IR frequency ω = 910 cm^{-1} (Figure S1) and 915 cm^{-1} (Figure S2) verified the twisting configuration of polaritons highlighted in the main text. Similar to Figure 1 in the main text, one can observe the polariton wavefront involve from open hyperbola (single slab and $\delta = 0^o$) to tilted hyperbola ($\delta = 20^o$), parenthesis ($\delta = 63^o$), oval ($\delta = 81^o$) and finally to squircle ($\delta = 90^o$) in Figures S1 and S2. These supplementary s-SNOM data further confirmed the wavefront configuration and topological transition of polaritons reported in the main text.

S2. s-SNOM image of twisted α-MoO_3 with $\delta = 90^o$ at 935 cm^{-1}

The s-SNOM image of twisted α-MoO_3 with $\delta = 90^o$ at IR frequency ω = 935 cm^{-1} is provided in Figure S3. This image is in accord with the data in Figure 3e in the main text and support our concluded criterion for the twisting configuration: while hyperbolic fringes are observed from both the top and bottom layer, they barely interact with each other.

S3. Fourier Transform of the s-SNOM image data

The Fourier Transform images of the s-SNOM data in Figure 1 of the main text are provided in Figure S4. These Fourier Transform images verified the topological transition from the open hyperbola-like geometry to the closed ellipse-like geometry.

S4. Real-space simulation of polaritons in twisted α-MoO_3

The real-space simulation of polaritons in twisted α-MoO_3 was performed with finite element method (FEM) using COMSOL Multiphysics. In the simulation, the twisted α-MoO_3 are modeled as closely-attached 3D slabs (simulation area = 15 μm × 15 μm) with the thicknesses input from our experiments. The bottom α-MoO_3 slab was aligned in the Cartesian system with [100] axis parallel to the x direction, the permittivity tensor is therefore $\bar{\bar{\varepsilon}}_{\mathrm{MoO_3}} = \mathrm{diag}[\varepsilon_x, \varepsilon_y, \varepsilon_z]$. The top α-MoO_3 slab was twisted with an angle δ, the permittivity tensor is $\bar{\bar{\varepsilon}}'_{\mathrm{MoO_3}} = U\bar{\bar{\varepsilon}}_{\mathrm{MoO_3}}U^T$, where

$$U = \begin{pmatrix} cos\delta & -sin\delta & 0 \\ sin\delta & cos\delta & 0 \\ 0 & 0 & 1 \end{pmatrix} \tag{S1}$$

is the transformation matrix. The twisted α-MoO_3 sits on the half infinite SiO_2 substrate and permittivity from ref.[1]. To excite the polaritons, we placed a linearly-polarized electric dipole along the z direction 100 nm above the top surface of the twisted α-MoO_3. The real part of the z component of the electric field Re(E_z) was extracted from the top surface of the twisted α-MoO_3 and plotted in Figure 2 in the main text. In Figure S1 we also provide the real-space simulation for s-SNOM data in Fig.3e in the main text.

The permittivity $\bar{\bar{\varepsilon}}_{\mathrm{MoO_3}}$ of α-MoO_3 can be described using the Lorentz oscillator:

$$\varepsilon_j(\omega) = \varepsilon_j^{\infty}\left(1+\frac{{\omega_j^{LO}}^2-{\omega_j^{TO}}^2}{{\omega_j^{TO}}^2-\omega^2-i\omega\Gamma_j}\right), j = x, y, z \tag{S2}$$

where $\varepsilon_j(\omega)$ is the component of $\bar{\bar{\varepsilon}}_{\mathrm{MoO_3}}$ at frequency ω, $\varepsilon_j^{\infty}=\varepsilon_j(\infty)$. The ω_j^{LO} and ω_j^{TO} are the longitude (LO) and transverse (TO) phonon frequencies, Γ_j is the damping constant. Due to the variety of the α-MoO_3 permittivity reported in the literature[2, 3], we adjust parameters in the Lorentz oscillator fit the real-space simulations to our s-SNOM data (Figure 1, main text). Our fitting yields ω_x^{LO} = 976 cm^{-1}, ω_x^{TO} = 816 cm^{-1}, Γ_x = 8 cm^{-1}, ε_x^{∞} = 4.8; ω_y^{LO} = 856 cm^{-1}, ω_y^{TO} = 542 cm^{-1}, Γ_y = 8 cm^{-1}, ε_y^{∞} = 5.2; ω_z^{LO} = 1012 cm^{-1}, ω_z^{TO} = 956 cm^{-1}, Γ_z = 8 cm^{-1}, ε_z^{∞} = 5.1. These parameters are supported by the previous literature[2, 3]. The dispersion of the α-MoO_3 permittivity has been plotted in Figure S8.

To further support the electromagnetic interaction as the origin of the polariton twisting configuration, in Figure S6 we provide the simulation results of polaritons in twisted α-MoO_3 with $\delta = 90^{\circ}$ where the top and bottom α-MoO_3 slabs were separated with a distance d_s (Fig. S6a). At small separation $d_s \leq 20$ nm in (Figs. S6b, c), polaritons exhibit a squircle wavefront due to the strong interaction between polaritons at the top and bottom α-MoO_3. As d_s increases (Figs. S6d-f), vertically aligned "X" shape polariton features appear and become evident. The "X" shape features originate from the basal plane hyperbolic response of top α-MoO_3 slab (Fig. S6g) and its appearance indicates the weaker electromagnetic interaction between polaritons in the top and bottom α-MoO_3 slab as d_s increases. As d_s further increase (d_s = 500nm in Fig. S6g), the electromagnetic interaction becomes negligible where the "X" shape wavefront dominates and is identical to that of the top α-MoO_3 only (Fig. S6g).

S5. Electromagnetic wave theory of polaritons in twisted α-MoO_3

As directional hyperbolic polaritons were mainly associated with the basal plane components

$\bar{\bar{\varepsilon}}_{\mathrm{MoO_3},xy} = \mathrm{diag}[\varepsilon_x, \varepsilon_y]$ of the permittivity tensor $\bar{\bar{\varepsilon}}_{\mathrm{MoO_3}}$, the α-$MoO_3$ slab can be modelled as an effective two-dimensional (2D) conductor with the conductivity tensor $\bar{\bar{\sigma}}_{\mathrm{s,MoO_3}}$ [4, 5]:

$$\bar{\bar{\sigma}}_{s,\mathrm{MoO_3}} = -i\omega d_t \cdot \bar{\bar{\varepsilon}}_{\mathrm{MoO_3},xy} \tag{S3}$$

where d_t is the thickness of the α-MoO_3 slab, we denote the thickness of the top and bottom α-MoO_3 slabs as d_{t1} and d_{t2}. To interpret the stacked α-MoO_3 slabs (Figure 1A in the main text), the two effective 2D conductors are separated by a distance d in the z direction (Fig. S7a). In our electromagnetic wave theory, the separation distance d is an adjustable parameter that can vary from 0 to $d_{\mathrm{total}}/2$, where $d_{\mathrm{total}} = d_{t1} + d_{t2}$.

In the twisting configuration, the effective conductivity needs to be processed with a series of coordinate transformation (Figs. S7b, c). We refer to the coordinate system aligned with the crystal axes of the bottom α-MoO_3 slab as *xyz*, where we have:

$$\bar{\bar{\sigma}}_{\mathrm{s,MoO_3},2} = \begin{bmatrix} \sigma_{xx,2} & 0 \\ 0 & \sigma_{yy,2} \end{bmatrix} \tag{S4}$$

The top α-MoO_3 slab rotate by an angle δ, we refer to the coordinate system aligned with the crystal axes of the top α-MoO_3 slab as *x'y'z* (Fig. S7b). For simplicity, here we define $\phi_0 = \delta + \pi/2$, where the azimuthal angle ϕ_0 is the angle between the $\hat{x}$ direction and $\hat{y}'$ direction in Fig. S7c. The conductivity of the top α-MoO_3 slab in the $x'y'z$ coordinates is:

$$\bar{\bar{\sigma}}'_{\mathrm{s,MoO_3},1} = \begin{bmatrix} \sigma_{x'x',1} & 0 \\ 0 & \sigma_{y'y',1} \end{bmatrix}. \tag{S5}$$

Through the coordinate transformation (see details in supplementary text 2), the conductivity of the top α-MoO_3 slab in xyz coordinates can be written as:

$$\bar{\bar{\sigma}}_{\mathrm{s,MoO_3},1} = \begin{bmatrix} \sigma_{x'x',1}\sin^2\phi_0 + \sigma_{y'y',1}\cos^2\phi_0 & (\sigma_{y'y',1} - \sigma_{x'x',1}) sin\phi_0 cos\phi_0 \\ (\sigma_{y'y',1} - \sigma_{x'x',1}) sin\phi_0 cos\phi_0 & \sigma_{x'x',1}\cos^2\phi_0 + \sigma_{y'y',1}\sin^2\phi_0 \end{bmatrix}. \tag{S6}$$

Without loss of generality, we assume polaritons in twisted α-MoO_3 propagate along the $\bar{k}_{\mathrm{in-plane}}$ direction in the xy plane. We further build the $x''y''z$ coordinates where $\bar{k}_{\mathrm{in-plane}} = \hat{x}'' k_{x''} = \hat{x}'' k_{\mathrm{in-plane}}$, and the azimuthal angle ϕ is the one between the $\hat{x}$ direction and $\hat{y}''$ direction (Fig. S7c).

In the xyz coordinates, we have

$$k_x = k_{\text{in-plane}} \cdot sin\phi, \quad k_y = -k_{\text{in-plane}} \cdot cos\phi. \tag{S7}$$

Again through the coordinate transformation, the conductivity of the top and bottom α-MoO_3 slab (S4, S6) in the $x''y''z$ coordinates is:

$$\bar{\bar{\sigma}}''_{\text{s,MoO}_3,1} = \begin{bmatrix} \sigma_{x'x',1}\sin^2(\phi-\delta)+\sigma_{y'y',1}\cos^2(\phi-\delta) & (\sigma_{x'x',1}-\sigma_{y'y',1})sin(\phi-\delta)cos(\phi-\delta) \\ (\sigma_{x'x',1}-\sigma_{y'y',1})sin(\phi-\delta)cos(\phi-\delta) & \sigma_{x'x',1}\cos^2(\phi-\delta)+\sigma_{y'y',2}\sin^2(\phi-\delta) \end{bmatrix} \tag{S8}$$

$$\bar{\bar{\sigma}}''_{\text{s,MoO}_3,2} = \begin{bmatrix} \sigma_{xx,2}\sin^2\phi+\sigma_{yy,2}\cos^2\phi & (\sigma_{xx,2}-\sigma_{yy,2})sin\phi cos\phi \\ (\sigma_{xx,2}-\sigma_{yy,2})sin\phi cos\phi & \sigma_{xx,2}\cos^2\phi+\sigma_{yy,2}\sin^2\phi \end{bmatrix} \tag{S9}$$

For simplicity, we denote $\bar{\bar{\sigma}}''_{\text{s,MoO}_3,1}$ and $\bar{\bar{\sigma}}''_{\text{s,MoO}_3,2}$ in equations (S8-9) as follows

$$\bar{\bar{\sigma}}''_{\text{s},1} = \bar{\bar{\sigma}}''_{\text{s,MoO}_3,1} = \begin{bmatrix} \sigma''_{xx,1} & \sigma''_{xy,1} \\ \sigma''_{xy,1} & \sigma''_{yy,1} \end{bmatrix} \tag{S10}$$

$$\bar{\bar{\sigma}}''_{\text{s},2} = \bar{\bar{\sigma}}''_{\text{s,MoO}_3,2} = \begin{bmatrix} \sigma''_{xx,2} & \sigma''_{xy,2} \\ \sigma''_{xy,2} & \sigma''_{yy,2} \end{bmatrix} \tag{S11}$$

The superscript $''$ both x and y is neglected in equations (S10-11) for simplicity.

In the $x''y''z$ coordinates, the electromagnetic boundary conditions at $z = 0$ (i.e., the location of the top 2D conductor) are:

$$\hat{\text{n}} \times (\bar{E}_1 - \bar{E}_2) = 0 \tag{S12}$$

$$\hat{\text{n}} \times (\bar{H}_1 - \bar{H}_2) = \bar{J}_{s,1} = \bar{\bar{\sigma}}''_{\text{s},1} \cdot \bar{E}_{1,at\ z=0}, \tag{S13}$$

where $\hat{n} = +\hat{z}$. Accordingly, the boundary conditions at $z = d_0$ (i.e., the location of the bottom 2D conductor) are:

$$\hat{\text{n}} \times (\bar{E}_2 - \bar{E}_3) = 0 \tag{S14}$$

$$\hat{\text{n}} \times (\bar{H}_2 - \bar{H}_3) = \bar{J}_{s,2} = \bar{\bar{\sigma}}''_{\text{s},2} \cdot \bar{E}_{1,at\ z=0}, \tag{S15}$$

where $d_0 = -d$ and d is the distance between the two effective 2D conductors.

With the conductivities and electromagnetic boundary conditions, we now proceed to derive the solution for polaritons in twisted α-MoO_3.

Due to the basal plane hyperbolicity, polaritons in α-MoO_3 are generally hybrid transverse magnetic-transverse electrical (TM-TE) eigenmodes. Without loss of generality, for the hybrid TM-TE eigenmodes, their total field can be written as the summation of field components of pure TM (i.e., *p*-polarized) waves and field components of pure TE (*s*-polarized) waves:

$$\bar{H}_{\text{total}} = \bar{H}_{TM} + \bar{H}_{TE} \tag{S16}$$

$$\bar{E}_{\text{total}} = \bar{E}_{TM} + \bar{E}_{TE}. \tag{S17}$$

For TM waves, in the $x''y''z$ coordinates, the fields in each region are:

$$\bar{H}_{TM,1} = \hat{y}'' e^{ik_{x''}x'' + ik_{z_1}z} \tag{S18}$$

$$\bar{E}_{TM,1,x} = \hat{x}'' \frac{-1}{\omega\varepsilon_1}\left(-k_{z_1}\right) e^{ik_{x''}x'' + ik_{z_1}z} \tag{S19}$$

$$\bar{H}_{TM,2} = \hat{y}'' \cdot \left(A_{TM,2}^{+} e^{+ik_{z_2}z} + A_{TM,2}^{-} e^{-ik_{z_2}z}\right) e^{ik_{x''}x''} \tag{S20}$$

$$\bar{E}_{TM,2,x} = \hat{x}'' \frac{-1}{\omega\varepsilon_2}\left(-k_{z_2} A_{TM,2}^{+} e^{+ik_{z_2}z} + k_{z_2} A_{TM,2}^{-} e^{-ik_{z_2}z}\right) e^{ik_{x''}x'' - ik_{z_2}z} \tag{S21}$$

$$\bar{H}_{TM,3} = \hat{y}'' \cdot A_{TM,3}^{-} e^{-ik_{z_3}z} e^{ik_{x''}x''} \tag{S22}$$

$$\bar{E}_{TM,3,x} = \hat{x}'' \frac{-1}{\omega\varepsilon_3}\left(+k_{z_3} A_{TM,3}^{-} e^{-ik_3 z}\right) e^{ik_{x''}x''}. \tag{S23}$$

Regions 1, 2 and 3 in Fig. S7a are above the top 2D conductor, between the two 2D conductors, and beneath the bottom 2D conductor, respectively. For the components of TE waves in the $x''y''z$ coordinates, the fields in each region are:

$$\bar{E}_{TE,1} = \hat{y}'' B_{TE,1}^{+} e^{ik_{x''}x'' + ik_{z_1}z} \tag{S24}$$

$$\bar{H}_{TE,1,x} = \hat{x}'' \frac{1}{\omega\mu_0}\left(-k_{z_1} B_{TE,1}^{+}\right) e^{ik_{x''}x'' + ik_{z_1}z} \tag{S25}$$

$$\bar{E}_{TE,2} = \hat{y}''(B_{TE,2}^{+} e^{+ik_{z_2}z} + B_{TE,2}^{-} e^{-ik_{z_2}z}) \cdot e^{ik_{x''}x''} \tag{S26}$$

$$\bar{H}_{TE,2,x} = \hat{x}'' \frac{1}{\omega\mu_0}\left(-k_{z_2} B_{TE,2}^{+} e^{+ik_{z_2}z} + k_{z_2} B_{TE,2}^{-} e^{-ik_{z_2}z}\right) e^{ik_{x''}x''} \tag{S27}$$

$$\bar{E}_{TE,3} = \hat{y}'' B_{TE,3}^{-} e^{ik_{x''}x'' - ik_{z_3}z} \tag{S28}$$

$$\bar{H}_{TE,3,x} = \hat{x}'' \frac{1}{\omega\mu_0}\left(+k_{z_3} B_{TE,3}^{-}\right) e^{ik_{x''}x'' - ik_{z_3}z}. \tag{S29}$$

Here $k_{z_j} = \sqrt{\frac{\omega^2}{c^2}\varepsilon_{rj} - k_{x''}^2}$ is the vertical wavevector component and ε_{rj} ($j = 1, 2$ or 3) are the relative permittivities of regions 1, 2 and 3, respectively. The seven unknown parameters of $A_{TM,2}^{+}$, $A_{TM,2}^{-}$, $A_{TM,3}^{+}$, $B_{TE,1}^{+}$, $B_{TE,2}^{+}$, $B_{TE,2}^{-}$ and $B_{TE,3}^{+}$, along with the unknown dispersion relation between $k_{x''}$ and ω, can be solved by matching the electromagnetic boundary conditions.

By enforcing the electromagnetic boundary conditions in equations (S12-15) and substituting the fields in equations (S18-29) into the boundary conditions, we have the following 8 linear equations:

$$-\frac{1}{\omega\varepsilon_1}(-k_{z1}) = -\frac{1}{\omega\varepsilon_2}\left(-k_{z2}A_{TM,2}^{+} + k_{z2}A_{TM,2}^{-}\right) \tag{S30}$$

$$B_{TE,1}^{+} = B_{TE,2}^{+} + B_{TE,2}^{-} \tag{S31}$$

$$-\left[1 - \left(\mathrm{A}_{\mathrm{TM},2}^{+} + \mathrm{A}_{\mathrm{TM},2}^{-}\right)\right] = \sigma_{xx,1}'' \cdot \left(-\frac{1}{\omega\varepsilon_1}\right)(-k_{z1}) + \sigma_{xy,1}'' B_{TE,1}^{+} \tag{S32}$$

$$+\left[\frac{1}{\omega\mu_0}(-k_{z1})B_{TE,1}^{+} - \frac{1}{\omega\mu_0}\left(-k_{z2}B_{TE,2}^{+} + k_{z2}B_{TE,2}^{-}\right)\right] = \sigma_{xy,1}'' \cdot \left(-\frac{1}{\omega\varepsilon_1}\right)(-k_{z1}) + \sigma_{yy,1}'' B_{TE,1}^{+} \tag{S33}$$

$$-\frac{1}{\omega\varepsilon_2}\left(-k_{z2}A_{TM,2}^{+}e^{ik_{z2}d_0}+k_{z2}A_{TM,2}^{-}e^{-ik_{z2}d_0}\right)=-\frac{1}{\omega\varepsilon_3}(+k_{z3})A_{TM,3}^{-}e^{-ik_{z3}d_0} \quad \text{(S34)}$$

$$B_{TE,2}^{+}e^{ik_{z2}d_0}+B_{TE,2}^{-}e^{-ik_{z2}d_0}=B_{TE,3}^{-}e^{-ik_{z3}d_0} \quad \text{(S35)}$$

$$-\left[\left(\mathrm{A}_{\mathrm{TM},2}^{+}e^{ik_{z2}d_0}+\mathrm{A}_{\mathrm{TM},2}^{-}e^{-ik_{z2}d_0}\right)-\mathrm{A}_{\mathrm{TM},3}^{-}e^{-ik_{z3}d_0}\right]=\sigma_{xx,2}''\cdot\left(\frac{-k_{z3}A_{TM,3}^{-}e^{-ik_{z3}d_0}}{\omega\varepsilon_3}\right)+\sigma_{xy,2}''B_{TE,3}^{-}e^{-ik_{z3}d_0} \quad \text{(S36)}$$

$$+\left[\frac{-k_{z2}B_{TE,2}^{+}e^{ik_{z2}d_0}+k_{z2}B_{TE,2}^{-}e^{-ik_{z2}d_0}}{\omega\mu_0}-\frac{k_{z3}B_{TE,3}^{-}e^{-ik_{z3}d_0}}{\omega\mu_0}\right]=\sigma_{xy,2}''\cdot\left(\frac{-k_{z3}A_{TM,3}^{-}e^{-ik_{z3}d_0}}{\omega\varepsilon_3}\right)+\sigma_{yy,2}''B_{TE,3}^{-}e^{-ik_{z3}d_0}\ . \quad \text{(S37)}$$

By solving equations (S30-37), we can get $A_{TM,2}^{+}$, $A_{TM,2}^{-}$, $A_{TM,3}^{+}$, $B_{TE,1}^{+}$, $B_{TE,2}^{+}$, $B_{TE,2}^{-}$ and $B_{TE,3}^{+}$, the dispersion relation between $k_{x''}$ and ω and the field distribution of polaritons in twisted α-MoO_3.

The dispersion for polaritons in twisted α-MoO_3 is written below:

$$\frac{P_3\cdot\sigma_{xy,2}''\cdot\frac{k_{z3}}{\omega\varepsilon_3}\cdot\frac{\omega\mu_0}{k_{z2}}\cdot\left(1+\frac{N_{2N}}{N_{2D}}\right)-P_4\cdot(M_{2N}-M_{2D})}{-P_1\cdot\sigma_{xy,2}''\cdot\frac{k_{z3}}{\omega\varepsilon_3}\cdot\frac{\omega\mu_0}{k_{z2}}\cdot\left(1+\frac{N_{2N}}{N_{2D}}\right)+P_3\cdot(M_{2N}-M_{2D})}=\frac{\mathrm{Q}_2\cdot\sigma_{xy,2}''\cdot\left(-1+\frac{M_{2N}}{M_{2D}}\right)-Q_4\cdot(N_{2N}+N_{2D})}{-\mathrm{Q}_1\cdot\sigma_{xy,2}''\cdot\left(-1+\frac{M_{2N}}{M_{2D}}\right)+Q_3\cdot(N_{2N}+N_{2D})} \quad \text{(S38)}$$

where

$$P_1=\sigma_{xy,1}''\cdot\left(e^{i2k_{z2}d_0}-1\right) \quad \text{(S39)}$$

$$P_2=M_{1D}e^{i2k_{z2}d_0}-M_{1N} \quad \text{(S40)}$$

$$P_3=N_{1D}e^{i2k_{z2}d_0}-N_{1N}\cdot\frac{N_{2N}}{N_{2D}} \quad \text{(S41)}$$

$$P_4=\sigma_{xy,1}''\cdot\frac{k_{z1}}{\omega\varepsilon_1}\cdot\frac{\omega\mu_0}{k_{z2}}\cdot\left(e^{i2k_{z2}d_0}+\frac{N_{2N}}{N_{2D}}\right) \quad \text{(S42)}$$

$$Q_1=N_{1D}e^{i2k_{z2}d_0}+N_{1N} \quad \text{(S43)}$$

$$Q_2=\sigma_{xy,1}''\cdot\frac{k_{z1}}{\omega\varepsilon_1}\cdot\frac{\omega\mu_0}{k_{z2}}\cdot\left(e^{i2k_{z2}d_0}-1\right) \quad \text{(S44)}$$

$$Q_3 = \sigma''_{xy,1} \cdot \left(e^{i2k_{z2}d_0} - \frac{M_{2N}}{M_{2D}}\right) \quad \text{(S45)}$$

$$Q_4 = M_{1D} e^{i2k_{z2}d_0} - M_{1N} \cdot \frac{M_{2N}}{M_{2D}} \quad \text{(S46)}$$

$$M_{1D} = 1 + \frac{k_{z1}/\varepsilon_1}{k_{z2}/\varepsilon_2} + \frac{k_{z1}}{\omega\varepsilon_1} \cdot \sigma''_{xx,1} \quad \text{(S47)}$$

$$M_{1N} = 1 - \frac{k_{z1}/\varepsilon_1}{k_{z2}/\varepsilon_2} + \frac{k_{z1}}{\omega\varepsilon_1} \cdot \sigma''_{xx,1} \quad \text{(S48)}$$

$$M_{2D} = 1 + \frac{k_{z3}/\varepsilon_3}{k_{z2}/\varepsilon_2} + \frac{k_{z3}}{\omega\varepsilon_3} \cdot \sigma''_{xx,2} \quad \text{(S49)}$$

$$M_{2N} = 1 - \frac{k_{z3}/\varepsilon_3}{k_{z2}/\varepsilon_2} + \frac{k_{z3}}{\omega\varepsilon_3} \cdot \sigma''_{xx,2} \quad \text{(S50)}$$

$$N_{1D} = 1 + \frac{k_{z1}}{k_{z2}} + \frac{\omega\mu_0}{k_{z2}} \cdot \sigma''_{yy,1} \quad \text{(S51)}$$

$$N_{1N} = 1 - \frac{k_{z1}}{k_{z2}} - \frac{\omega\mu_0}{k_{z2}} \cdot \sigma''_{yy,1} \quad \text{(S52)}$$

$$N_{2D} = 1 + \frac{k_{z3}}{k_{z2}} + \frac{\omega\mu_0}{k_{z2}} \cdot \sigma''_{yy,2} \quad \text{(S53)}$$

$$N_{2N} = 1 - \frac{k_{z3}}{k_{z2}} - \frac{\omega\mu_0}{k_{z2}} \cdot \sigma''_{yy,2} \quad \text{(S54)}$$

$$\sigma''_{xx,1} = \sigma_{x'x',1} \sin^2(\phi - \delta) + \sigma_{y'y',1} \cos^2(\phi - \delta) \quad \text{(S55)}$$

$$\sigma''_{xy,1} = \left(\sigma_{x'x',1} - \sigma_{y'y',1}\right) sin(\phi - \delta) cos(\phi - \delta) \quad \text{(S56)}$$

$$\sigma''_{yy,1} = \sigma_{x'x',1} \cos^2(\phi - \delta) + \sigma_{y'y',2} \sin^2(\phi - \delta) \quad \text{(S57)}$$

$$\sigma''_{xx,2} = \sigma_{xx,2} \sin^2 \phi + \sigma_{yy,2} \cos^2 \phi \quad \text{(S58)}$$

$$\sigma''_{xy,2} = (\sigma_{xx,2} - \sigma_{yy,2}) sin\phi cos\phi \tag{S59}$$

$$\sigma''_{yy,2} = \sigma_{xx,2}\cos^2\phi + \sigma_{yy,2}\sin^2\phi. \tag{S60}$$

The isofrequency contour of polaritons in twisted α-MoO_3 can be obtained by solving equation (S38) with equation (S7), and $k_{z_j} = \sqrt{\frac{\omega^2}{c^2}\varepsilon_{rj} - k^2_{\text{in-plane}}}$.

For highly confined polaritons, the lengthy equation (S38) can be re-organized into an intuitive way as follows:

$$\left(N_{1D}N_{2D}e^{i2k_{z2}d_0} - N_{1N}N_{2N}\right)\cdot\left(M_{1D}M_{2D}e^{i2k_{z2}d_0} - M_{1N}M_{2N}\right) = f(\sigma''_{xy,1}, \sigma''_{xy,2}) \ , \tag{S61}$$

where $f(\sigma''_{xy,1}, \sigma''_{xy,2})$ represents all terms in equation (S38) that contain $\sigma''_{xy,1}$ or $\sigma''_{xy,2}$. The term $\left(N_{1D}N_{2D}e^{i2k_{z2}d_0} - N_{1N}N_{2N}\right)$ is directly related to pure TE waves, while the term $\left(M_{1D}M_{2D}e^{i2k_{z2}d_0} - M_{1N}M_{2N}\right)$ is directly related to pure TM waves. The nonzero $f(\sigma''_{xy,1}, \sigma''_{xy,2})$ in equation (S61) indicates polaritons in twisted α-MoO_3 are hybrid TE-TM waves.

According to ref.[6], for highly-confined hybrid TM-TE polaritons in non-magnetic systems, the TM component dominates. In equation (S61), we have:

$$\left|\frac{f(\sigma''_{xy,1}, \sigma''_{xy,2})}{\left(N_{1D}N_{2D}e^{i2k_{z2}d_0} - N_{1N}N_{2N}\right)}\right| \ll 1 \tag{S62}$$

Then for highly confined polaritons, equation (S62) can be reduced to

$$\left(M_{1D}M_{2D}e^{i2k_{z2}d_0} - M_{1N}M_{2N}\right) = 0 \tag{S63}$$

By substituting $d_0 = -d$:

$$\left(M_{1D}M_{2D}e^{-i2k_{z2}d} - M_{1N}M_{2N}\right) = 0 \ , \tag{S64}$$

The iso-frequency contours in Figure 2 of the main text are plotted based on equation (S64) with d = 5 nm (δ = 0°, ω = 915 cm^{-1}, d_{t1} = 240 nm and d_{t2} = 229 nm) in Figure 2b, bottom, d = 5 nm (δ = 20°, ω = 910 cm^{-1}, d_{t1} = 234 nm and d_{t2} = 178 nm) in Figure 2c, bottom, d = 3 nm (δ = 63°,

ω = 920 cm^{-1}, d_{t1} =163 nm and d_{t2} = 176 nm) in Figure 2d, bottom, d = 6 nm (δ = 81°, ω = 915 cm^{-1}, d_{t1} = 191 nm and d_{t2} = 242 nm) in Figure 2e, bottom and d = 15 nm (δ = 90°, ω = 905 cm^{-1}, d_{t1} = 137 nm and d_{t2} = 168 nm) in Figure 2f, bottom. The separation distance d various a bit with the thicknesses of the α-MoO_3 slabs and the IR frequency ω.

In Movie S1, we show the detailed evolution of the isofrequency curve as a function of the twisting angle δ, where the configuration of the wavefront and topological transition can be observed.

S6. Thickness dependence of polaritons in twisted α-MoO_3

In Figure S9, we provide the thickness dependence results of polaritons in twisted α-MoO_3 via both FEM simulation (Figures S9, top panels) and electromagnetic theory (Figure S9, bottom panels) at a representative twisting angle δ = 90° and frequency ω = 900 cm^{-1}. The real-space FEM simulation images reveal the strong dependence of the polariton wavefront geometry on the thicknesses of the top (d_{top}) and bottom (d_{bot}) slab. For structures where d_{top} and d_{bot} are significantly different (Figures S9a,b,e,f, top), the thicker slab dominates the polariton wavefront geometry in twisted α-MoO_3. Our electromagnetic theory (Section S5) also show thickness dependence (Figure S9, bottom panels) in the k-space and are in accord with those from FEM.

S7. Frequency-momentum dispersion in twisted α-MoO_3 and single slab α-MoO_3

The dispersion of twisted α-MoO_3 with 170nm-thick top and bottom α-MoO_3 slab at the twisting angle δ = 90° and the dispersion of the bottom α-MoO_3 slab only are plotted in Figure S10. At frequencies ω < 930 cm^{-1}, the dispersion of twisted α-MoO_3 (Figures S10a, c) and bottom α-MoO_3 (Figures S10b, d) are distinctly different: the isofrequency curves from the twisted α-MoO_3 appear as squircles or ellipses while those from bottom α-MoO_3 are always hyperbolas. At ω > 930 cm^{-1}, the dispersion become related: isofrequency curves from twisted α-MoO_3 are approximated as superpositioned hyperbolas (Figure S10c) of the curves in the bottom α-MoO_3 (Figure S10d) and their 90° twist. The dispersion plots in Figure S10 are in accord with our experimental results in Figures 1, 3 of the main text and Figure S3: at ω < 930 cm^{-1}, evident twisting configuration of polaritons can be observed, hyperbolic polaritons from the bottom and top strongly couple with each other and lead to new wavefront (Figure 3f), whereas at ω > 930 cm^{-1}, these hyperbolic polaritons superposition but barely couple with each other (Figures 3e and S3). We also note a topological transition is observed in twisted α-MoO_3 (Figures S10a, c) as the ω increases but is absent in the bottom α-MoO_3 slab (Figures S10b, d).

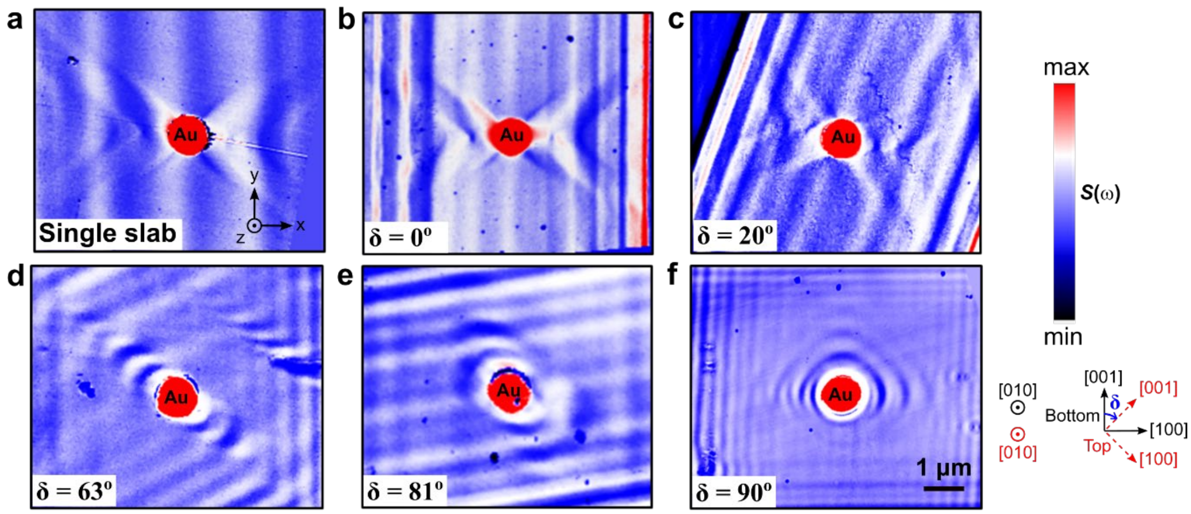

Figure S1 | s-SNOM amplitude images of polaritons in single slab α-MoO_3 and twisted α-MoO_3 slabs at ω = 910cm^{-1}. **a**, Single slab. **b**, δ= 0°. **c**, δ= 20°. **d**, δ= 63°. **e**, δ= 81°. **f**, δ= 90°. Scale bar: 1 μm.

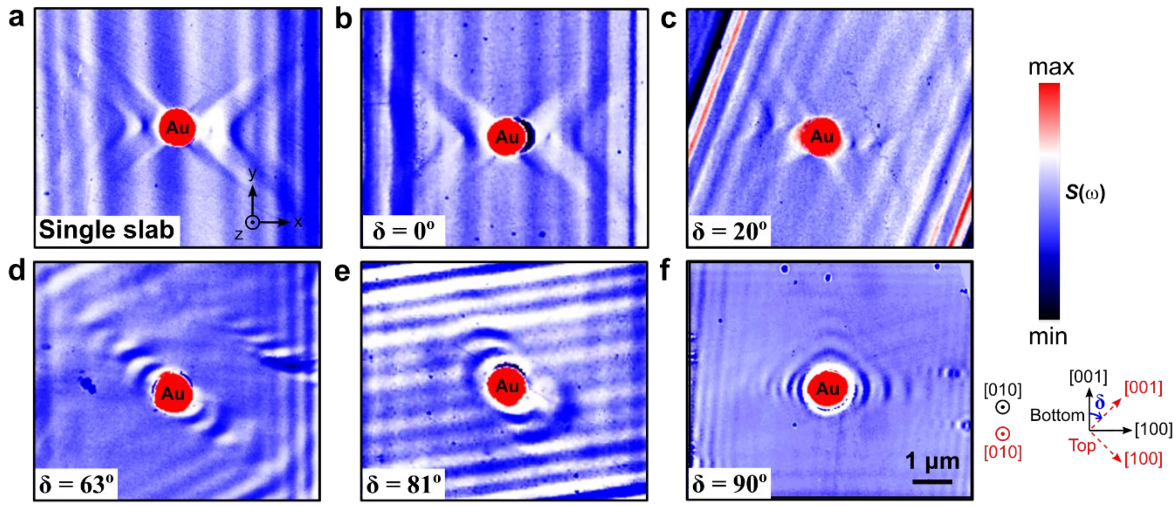

Figure S2 | s-SNOM amplitude images of polaritons in single slab α-MoO_3 and twisted α-MoO_3 slabs at ω = 915cm^{-1}. a, Single slab. **b**, δ = 0°. **c**, δ = 20°. **d**, δ = 63°. **e**, δ = 81°. **f**, δ = 90°. Scale bar: 1 μm.

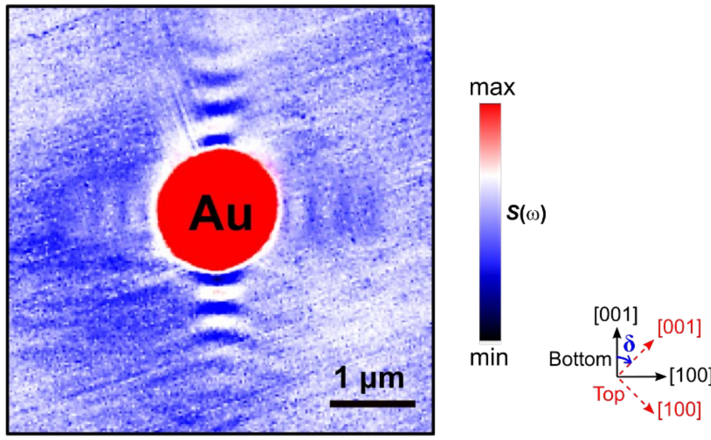

Figure S3 | s-SNOM amplitude image of polaritons in twisted α-MoO_3 with δ = 90º at ω = 935cm^{-1}. Scale bar: 1 µm.

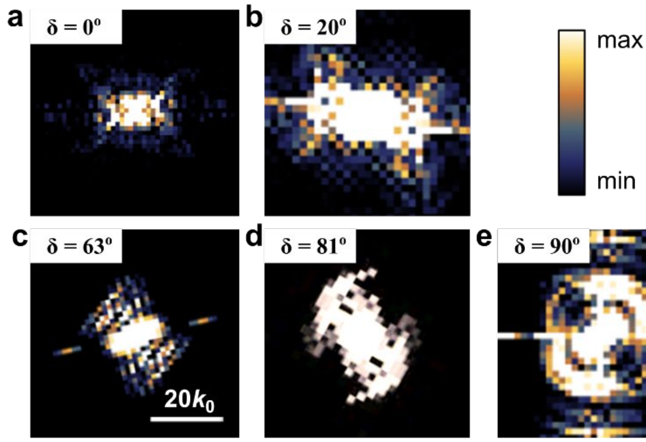

Figure S4 | Fourier Transform image of the s-SNOM data in Figure 1 of the main text.

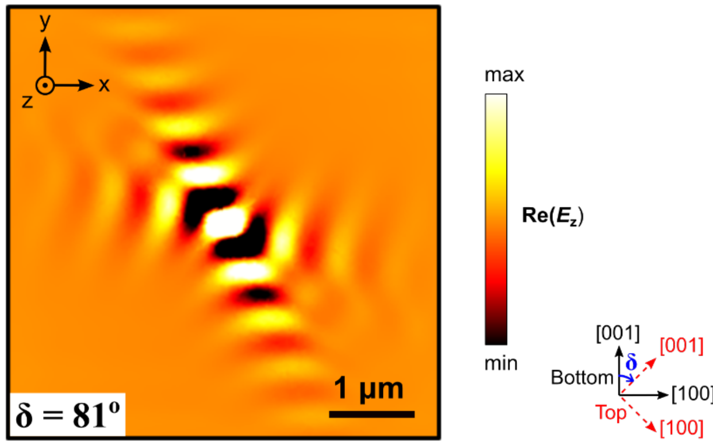

Figure S5 | Real-space simulation of twisted α-MoO_3 slabs (δ = 81°) at ω = 935 cm^{-1}. Scale bar: 1μm.

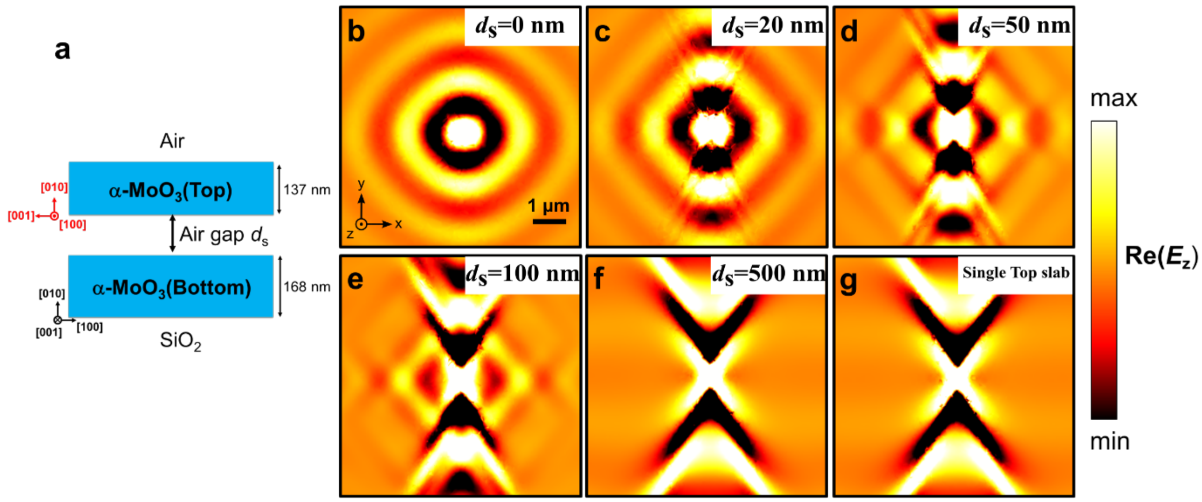

Figure S6 | Simulation of polaritons in twisted α-MoO_3 where top and bottom α-MoO_3 were separated with d_s. a, Schematic illustration. The dipole source is put 100 nm above the surface of top α-MoO_3 slab. **b -g**, Real-space Re($\boldsymbol{E}_z$) map of polaritons at different gap distance d_s = 0 nm (**b**), 20 nm (**c**), 50 nm (**d**), 100 nm (**e**), 500 nm (**f**) and single top slab (**g**). IR frequency ω = 900 cm^{-1}, thickness of the top and bottom α-MoO_3: 100 nm. Scale bar: 1 μm.

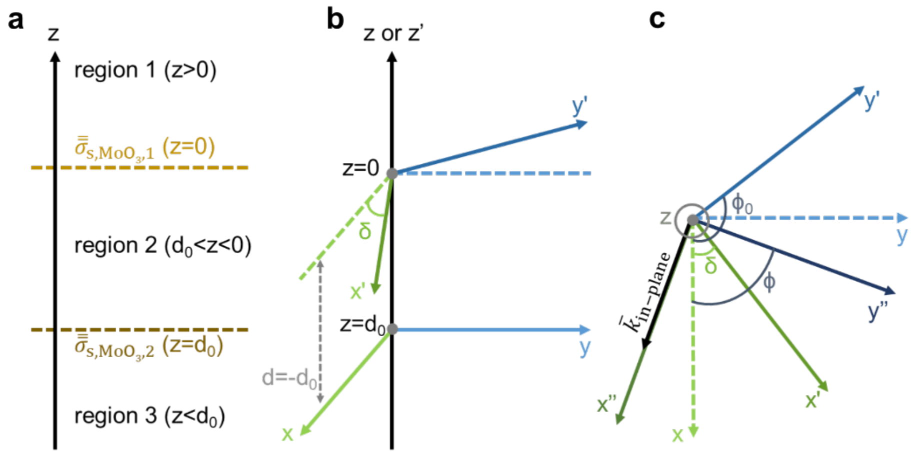

Figure S7 | Schematic of the structural setup in the analytical calculation. a, The two effective surface conductivities of α-MoO_3 slabs are separated by a distance *d*, where d=-d_0 Region 1 is free space. For simplicity, the dielectric region 2 can be treated as free space. Region 3 is the dielectric substrate. **b**, The top α-MoO_3 slab is rotated by an angle δ with respect to the bottom α-MoO_3 slab. **c**, Relation between different coordinates used in the analytical calculation in the *xy* plane. For these self-defined coordinates, they share the same*z* axis.

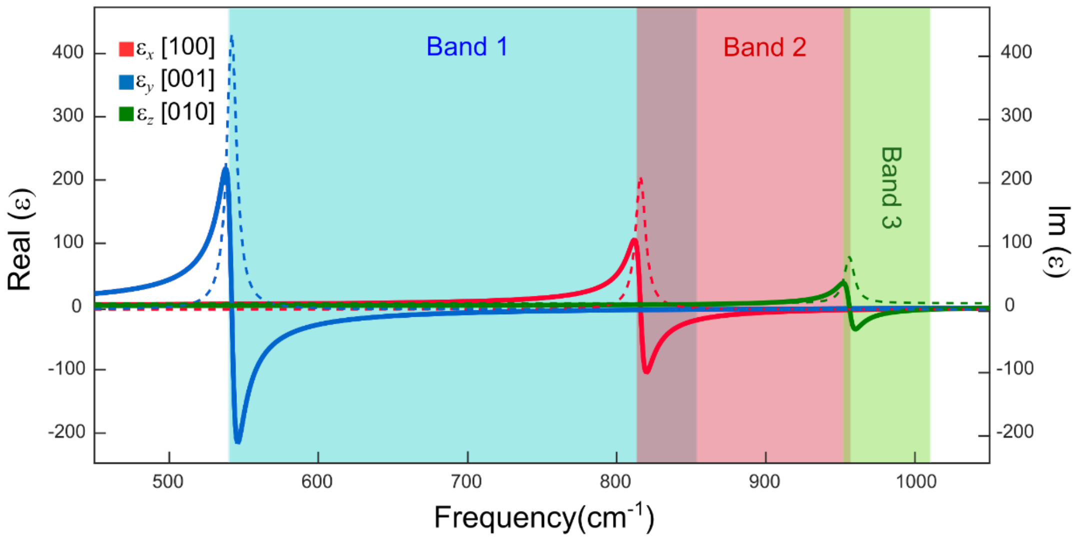

Figure S8 | Permittivity of α-MoO_3. Real (ε) is plotted in solid curve while Im (ε) is plotted in dashed curve.

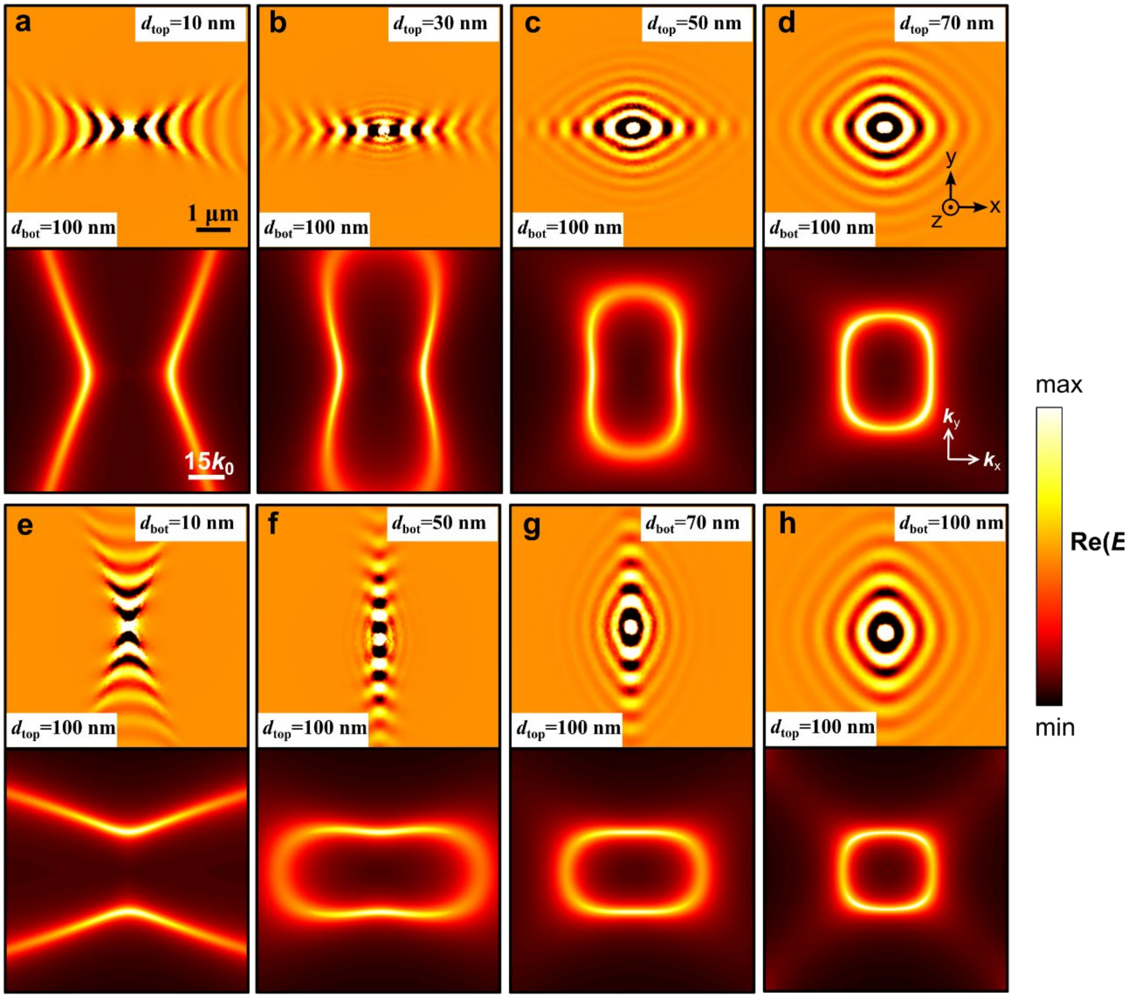

Figure S9 | Thickness dependence of polaritons in twisted α-MoO_3 (δ = 90°) revealed by both FEM simulation and electromagnetic theory at ω = 900 cm^{-1}. d_{top} and d_{bot} denote the thickness of the top and bottom α-MoO_3 slab.

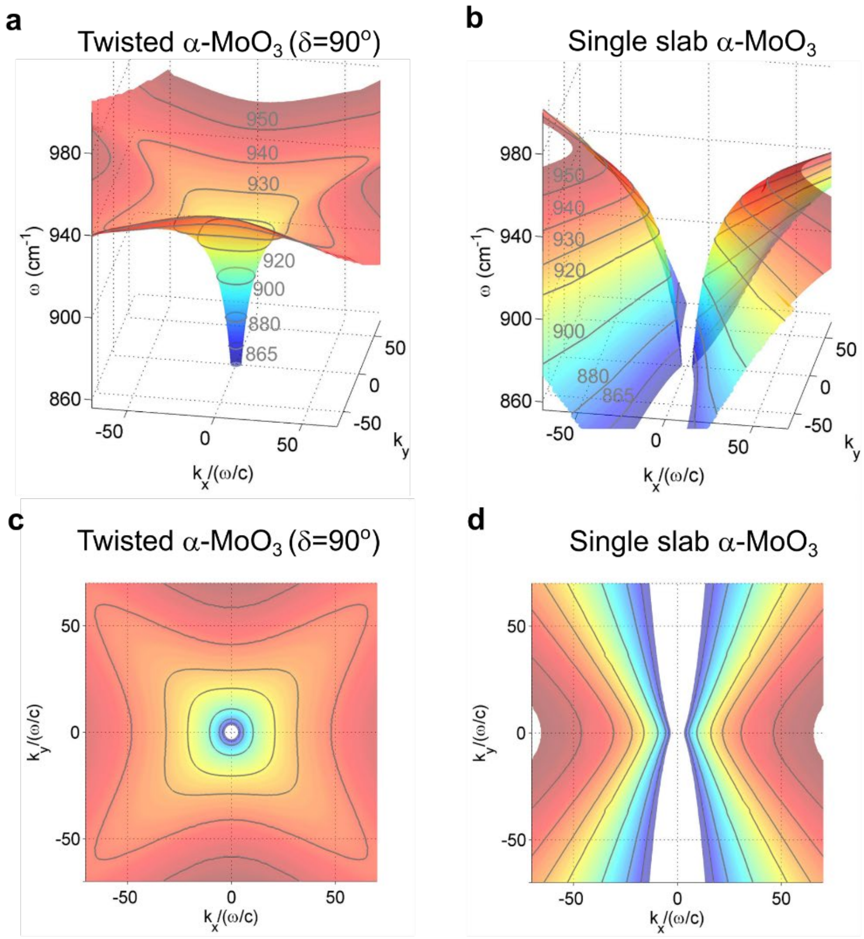

Figure S10 | Dispersion of twisted and single slab α-MoO_3. a, Dispersion of twisted α-MoO_3 with $\delta = 90^o$, top and bottom slab thickness both at 170 nm. **b,** Dispersion of single slab α-MoO_3 with the thickness at 170 nm. **c,d,** The top view of (**a**) and (**b**), respectively. The isofrequency contours of phonon polaritons at representative frequencies are also tracked with black lines. These panels were plotted based on the electromagnetic wave theory (Section S5). For clarity, only fundamental polariton branches are plotted. Color in all panels denotes the frequency ω.

Movie 1

k-space isofrequency curve of twisted α-MoO_3 in the range of 0º to 180º.

References

1. Palik ED. *Handbook of Optical Constants of Solids* Academic Press (1985).

2. Zheng Z*, et al.* A mid-infrared biaxial hyperbolic van der Waals crystal. *Sci Adv* **5**, eaav8690 (2019).

3. Álvarez-Pérez, G. et al. Infrared Permittivity of the Biaxial van der Waals Semiconductor α-MoO3 from Near- and Far-Field Correlative Studies. *Advanced Materials*, 1908176 (2020).

4. Ma W*, et al.* In-plane anisotropic and ultra-low-loss polaritons in a natural van der Waals crystal. *Nature* **562**, 557-562 (2018).

5. Vakil A, Engheta N. Transformation optics using graphene. *Science* **332**, 1291-1294 (2011).

6. Jiang J, Lin X, Zhang B. Broadband Negative Refraction of Highly Squeezed Hyperbolic Polaritons in 2D Materials. *Research (Wash D C)* **2018**, 2532819 (2018).